Supporting Information for "Global three-dimensional water vapor feature-tracking for horizontal wind using hyper-spectral infrared sounder data from overlapped tracks of two satellites"

Amir Ouyed [1], Nadia Smith[2], Xubin Zeng[1], Thomas Galarneau, Jr. [3,4], Hui Su[5], and Ross D. Dixon[6]

[1]Department of Hydrology and Atmospheric Sciences, University of Arizona, Tucson, Arizona

[2]Science and Technology Corporation, Columbia, Maryland

[3]Cooperative Institute for Severe and High-Impact Weather Research and Operations, University of Oklahoma

[4]NOAA/OAR National Severe Storms Laboratory, Norman, Oklahoma

[5] Department of Atmospheric and Oceanic Sciences, University of California—Los Angeles, Los Angeles, California

[6]Department of Earth and Atmospheric Sciences, University of Nebraska—Lincoln, Lincoln, Nebraska

Contents of this file

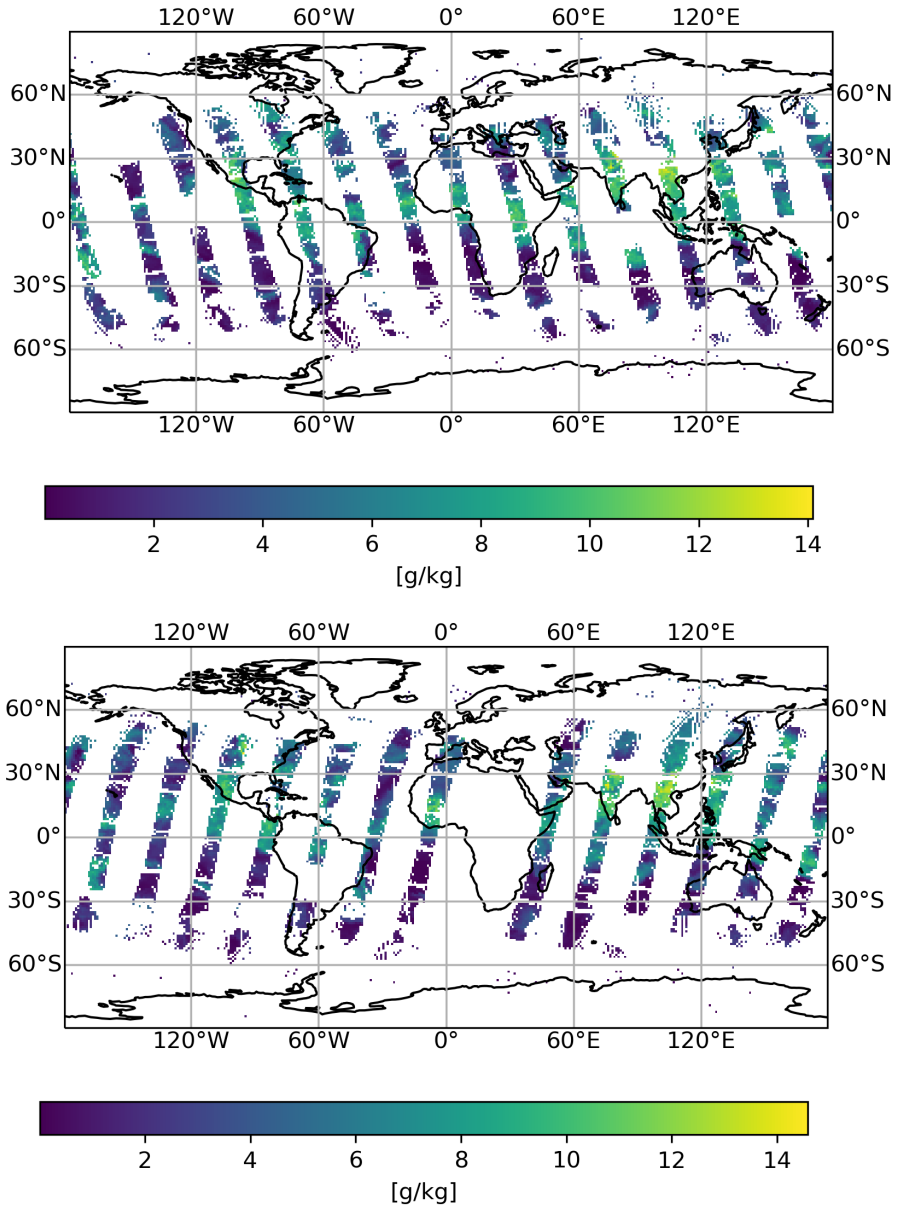

Figure S1. Humidity overlapping tracks used to calculate AMVs from the original 49 levels (as opposed to the post-processed 9 levels) for P=706 hPa, July 1, 2020 for ascending orbit (s), and descending orbit (b). Gap in 0-30E in (b) is due to the fact that the track corresponds to the next day in UTC.

f

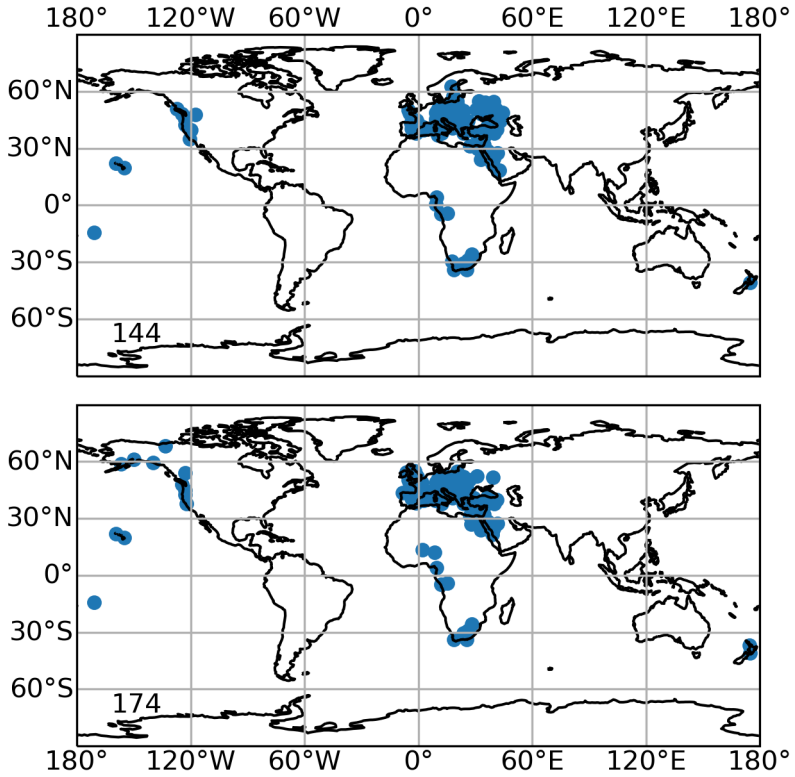

Figure S2. Locations of radiosonde stations used to collocate AMVs. Panel (a) is the map for January 1-7, 2020 and panel (b) is for July 1-7, 2020. The quantity in the lower left of each panel is for the total number of radiosonde profiles used.

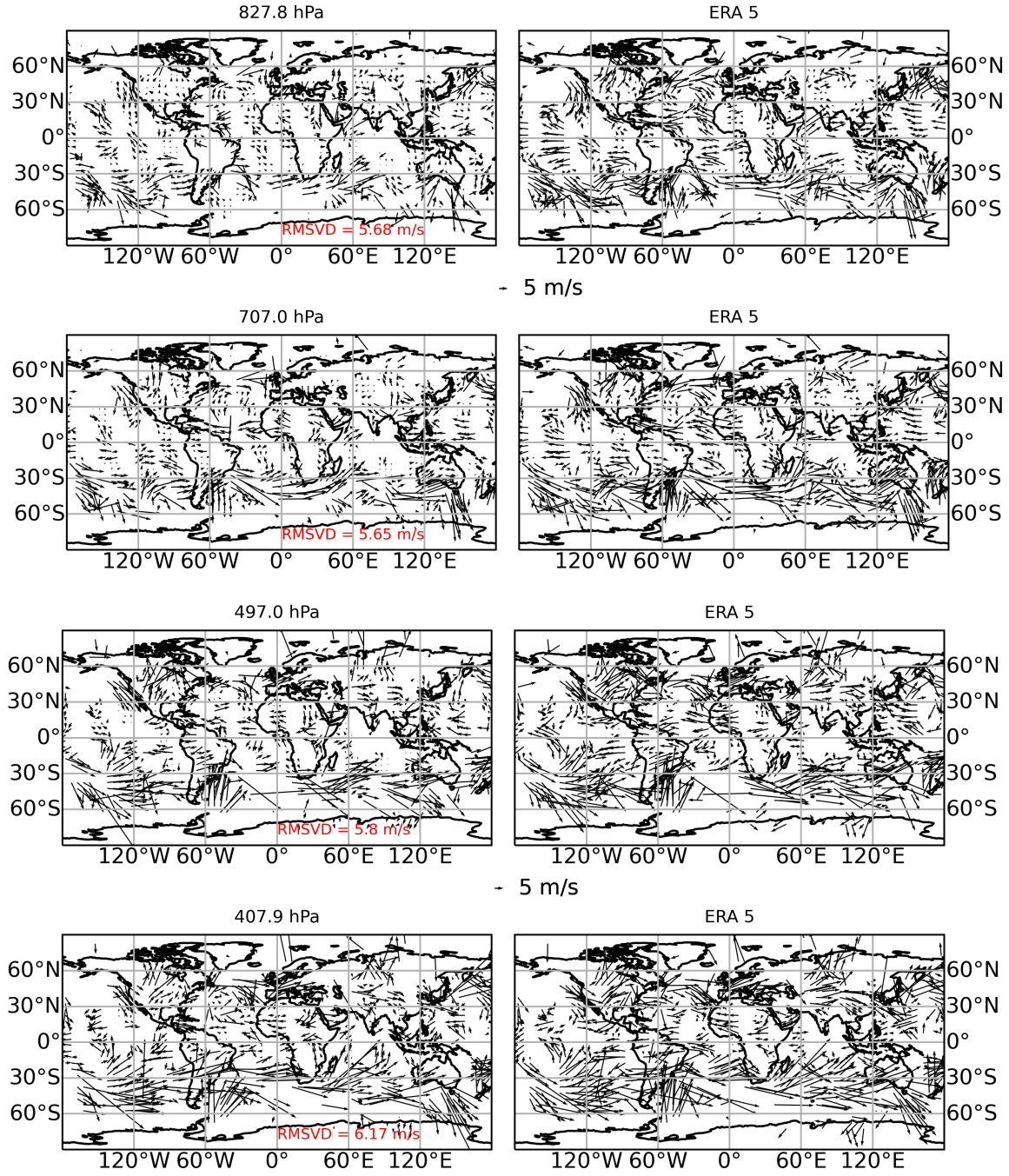

Figure S3. Retrieved horizontal wind for the ascending orbit of July 1, 2020 for different pressure levels in left panels. The corresponding results from ERA-5 are shown in right panels. Resolution averaged to 5° to make the plot readable. Root Mean Square Vector Difference (RMSVD) in left panels computed at the original horizontal resolution of 1°.

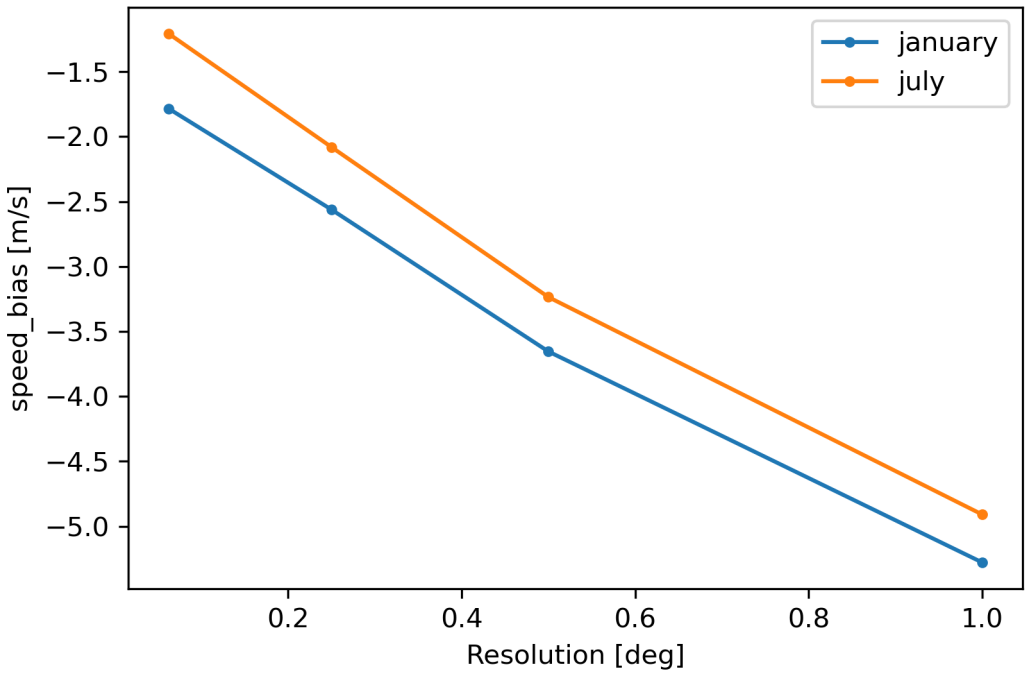

Figure S4. Speed bias versus resolution (deg) for AMVs computed from GEOS 5 Nature Run for P=500 hPa, dt=60 mins, and the first three days of January 2016 and July 2016. AMVs were calculated for 0:00, 6:00, 12:00, 18:00 using the Open-CV implementation of deepflow for the optical flow algorithm from Ouyed et al. 2021.

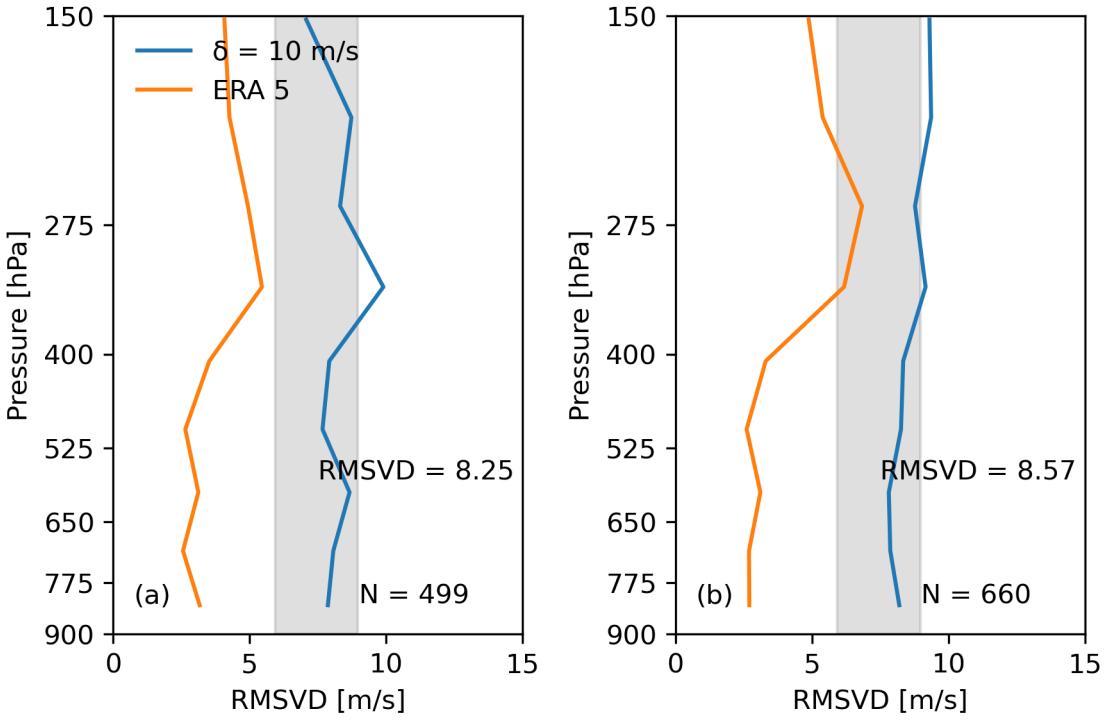

Figure S5. Same as Fig. 3a,b but for random vectors.

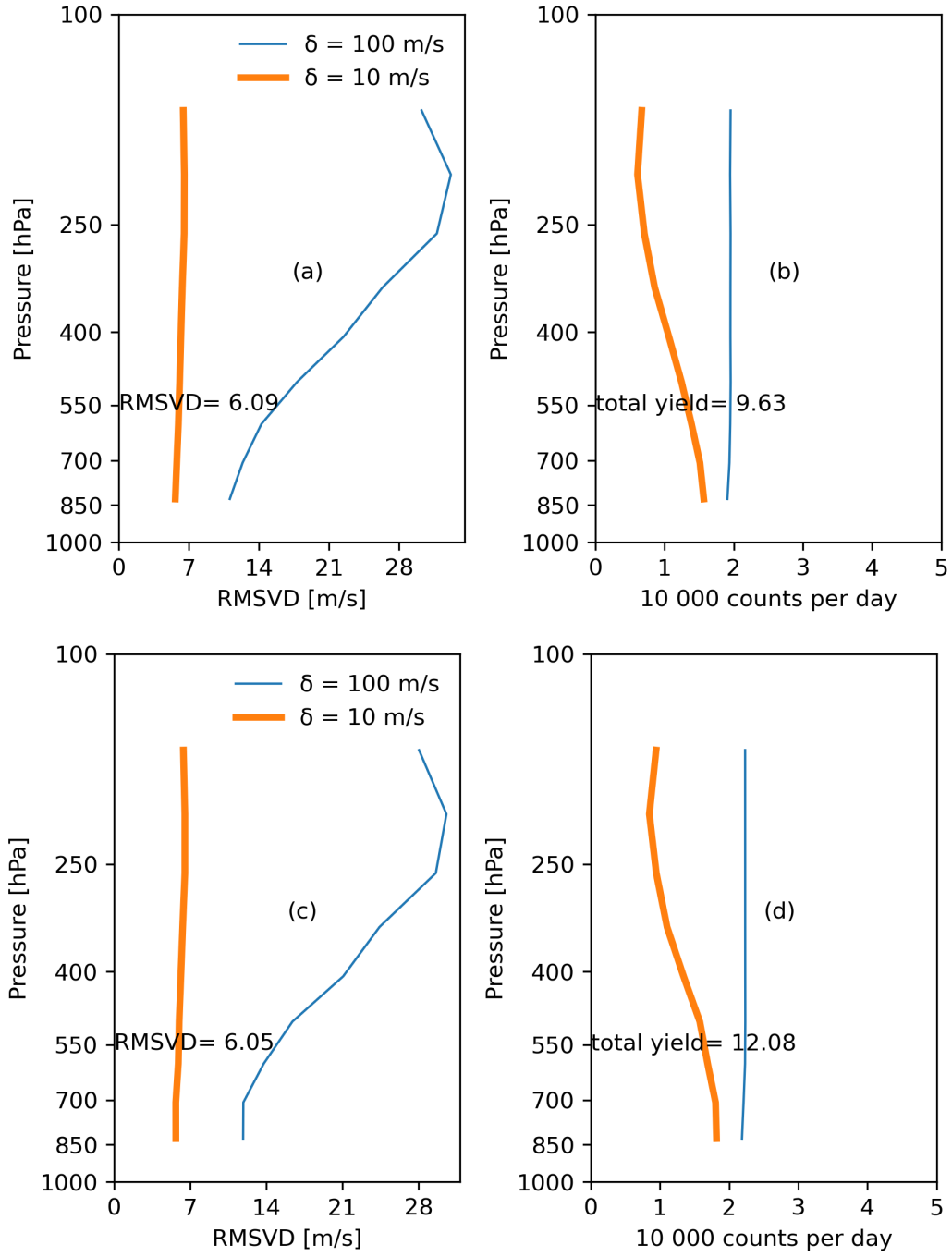

Figure S6. RMSVD between retrieved AMVs and ERA-5 results versus pressure in (a), and 3D AMV counts per day versus pressure in (b) for January 1-7, 2020. Panels (c) and (d) are same as (a) and (b) except for July 1-7, 2020. No error check was done for $\delta = 100$ m s^{-1}. The RMSVDs averaged at nine levels are provided in panels (a) and (c), while the total counts at all nine levels per day are provided in (b) and (d).

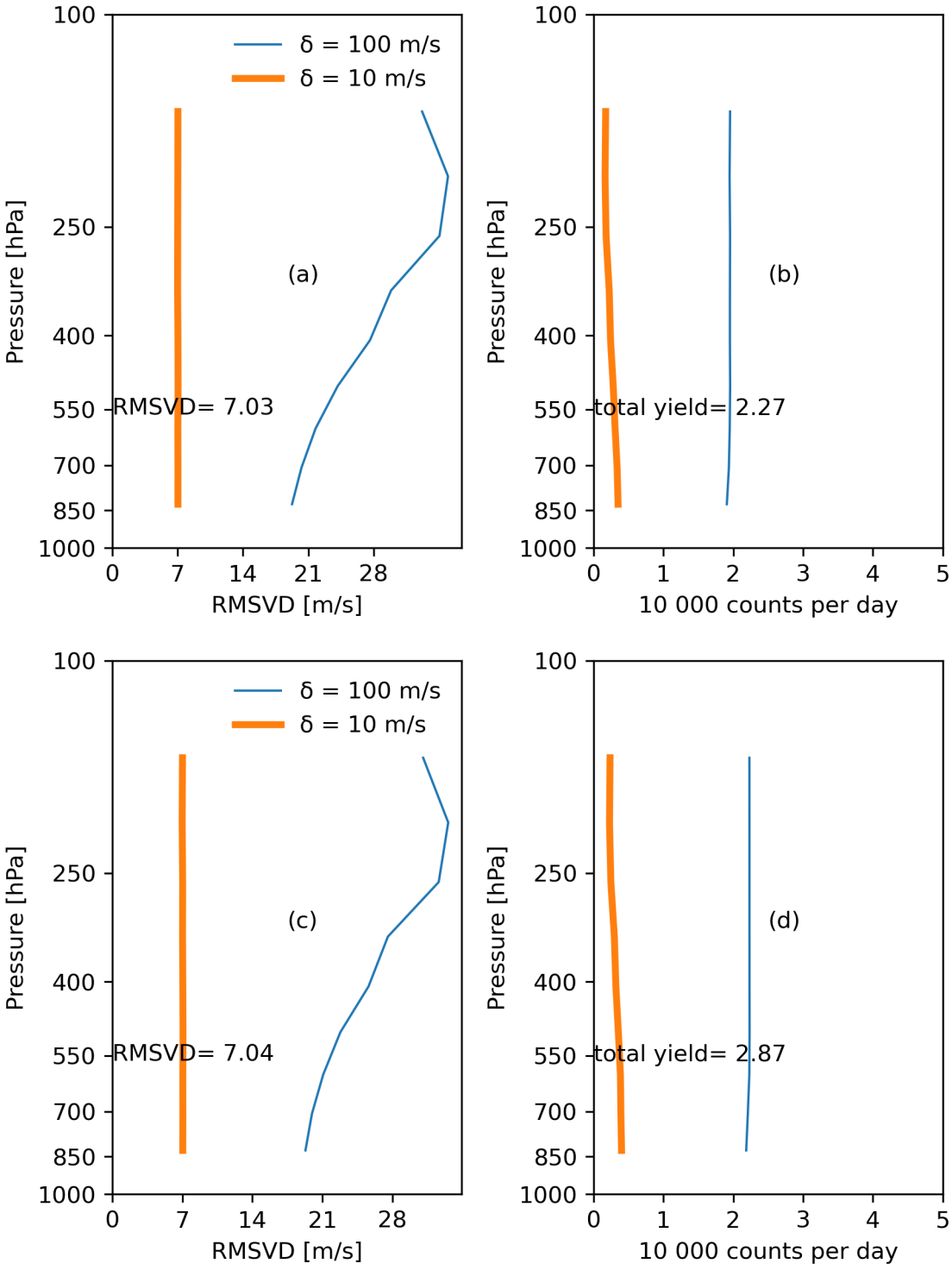

Figure S7. Same as Fig. S6 but for random vectors.

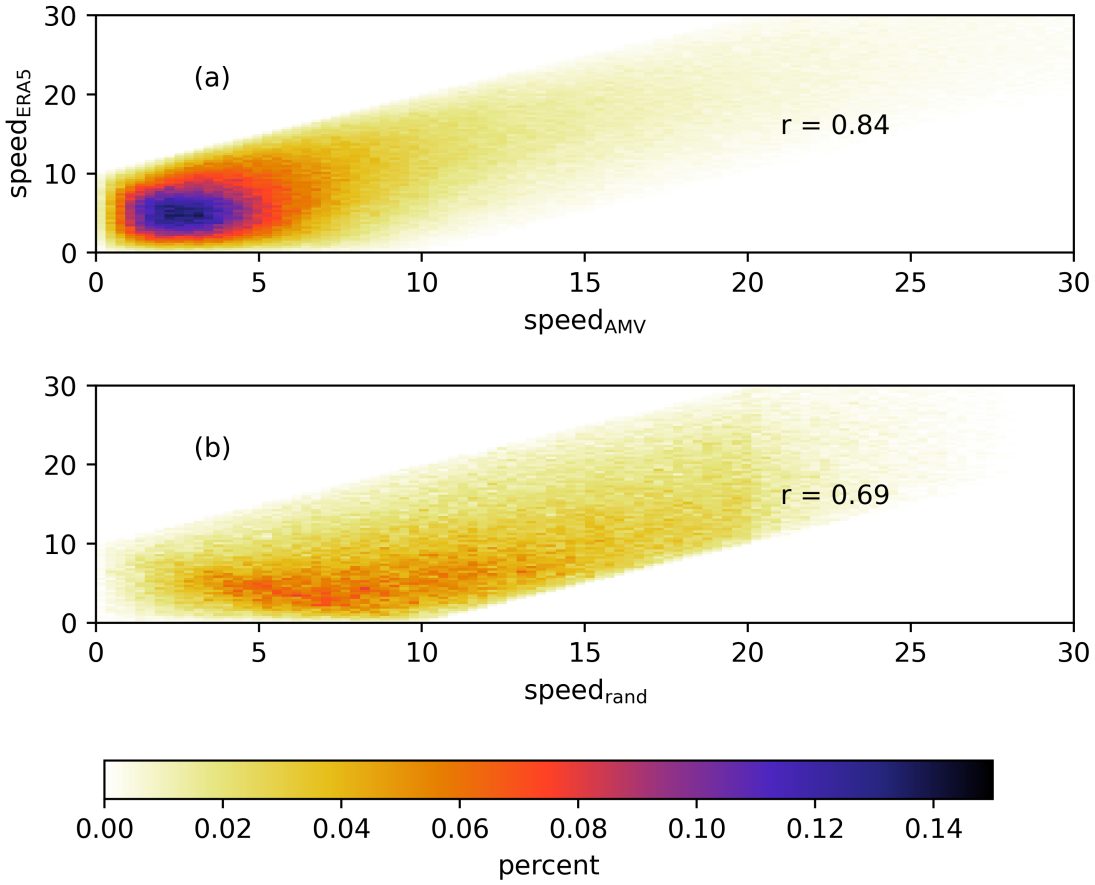

Figure S8. Histograms (percentage of grids) of ERA-5 wind speeds versus AMVs in (a) and random vector speeds post-processed for error check in (b) for January 1-7, 2020. The Pearson correlation coefficient r is displayed on each panel.